COSMOLOGICAL CONSTRAINTS ON VARIATIONS OF FINE STRUCTURE CONSTANT FROM CMB DATA

Ph.D student Eloisa Menegoni
Eloisa.menegoni@roma1.infn.it
ICRA, University of Rome “Sapienza”

The XI-th School of Cosmology 17-22 of September 2012

CMB anisotropies

$$\left\langle \frac{\Delta T}{T}(\vec{\gamma}_1)\frac{\Delta T}{T}(\vec{\gamma}_2)\right\rangle = \frac{1}{2\pi}\sum_{\ell}(2\ell+1)\,C_\ell\,P_\ell(\vec{\gamma}_1\cdot\vec{\gamma}_2)$$

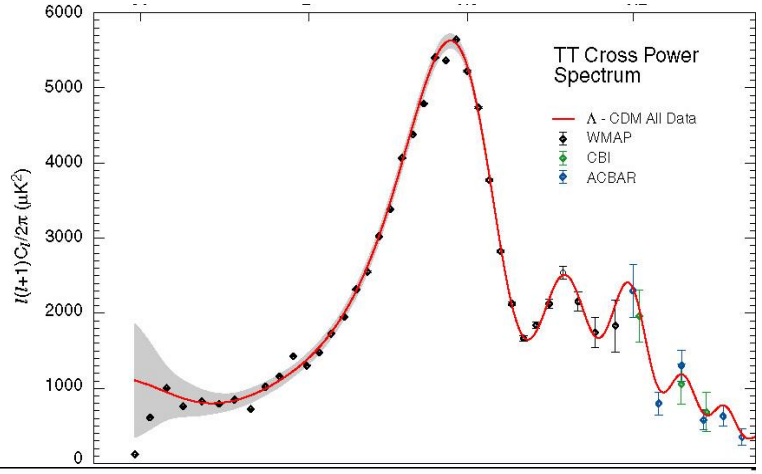

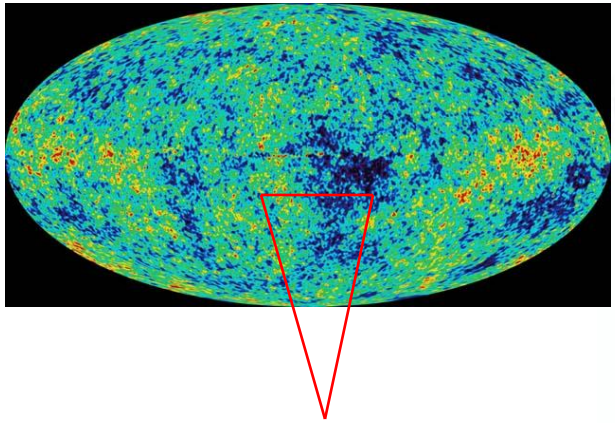

$$\vartheta \approx 1/l$$

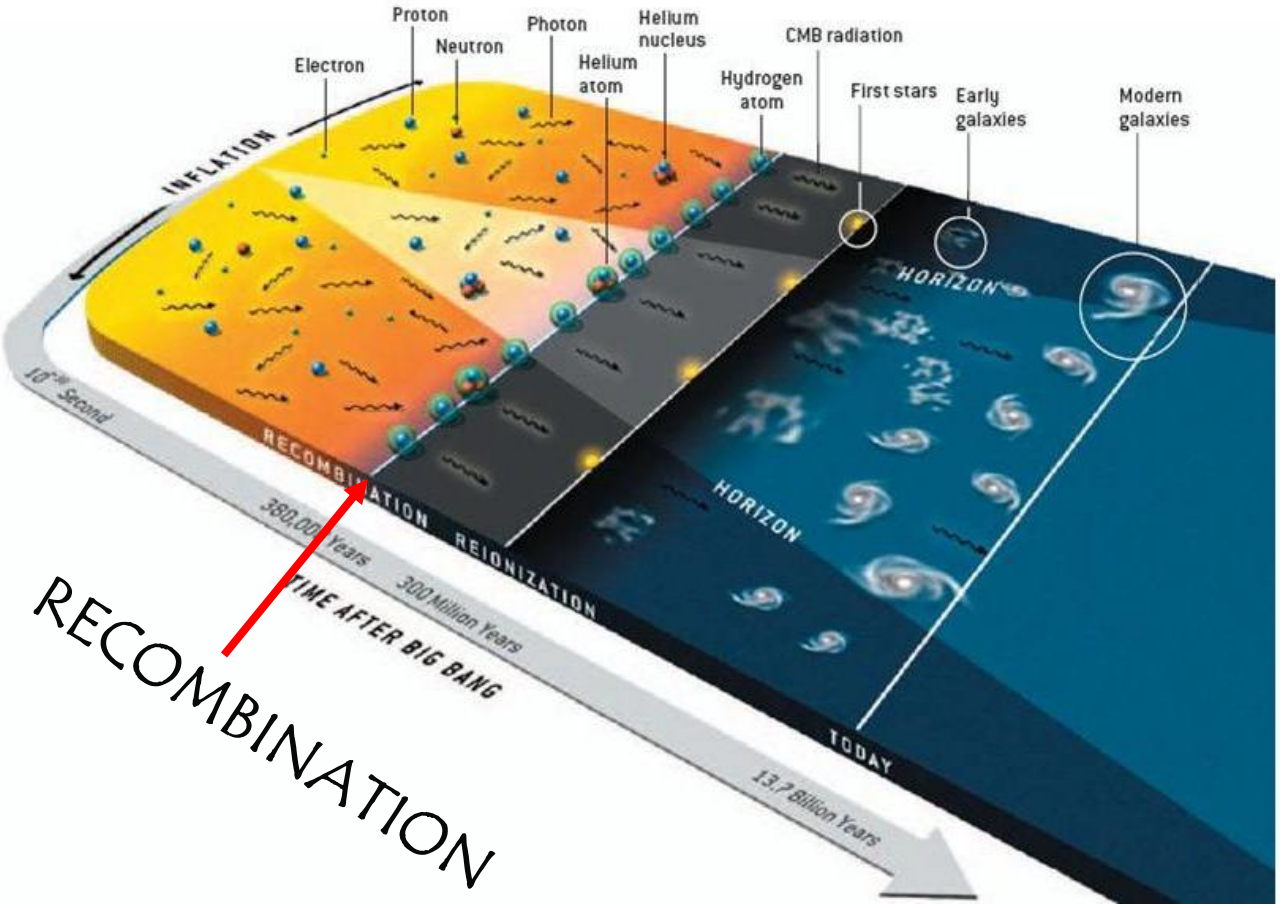

RECOMBINATION

The CMB Angular Power Spectrum

The main reason of this success relies on the existance of a highly predictable theoretical model that describes the CMB anisotropies.
The most important theoretical prediction is the CMB anisotropy angular power spectrum.
i.e. you consider a two point correlation function For the anisotropies in the sky, you expand the correlation function in Legendre polinomials (i.e. there is non azimuthal dependence for The anisotropies) and the model predict a value of the Legendre coefficient in function of the order l as in figure.

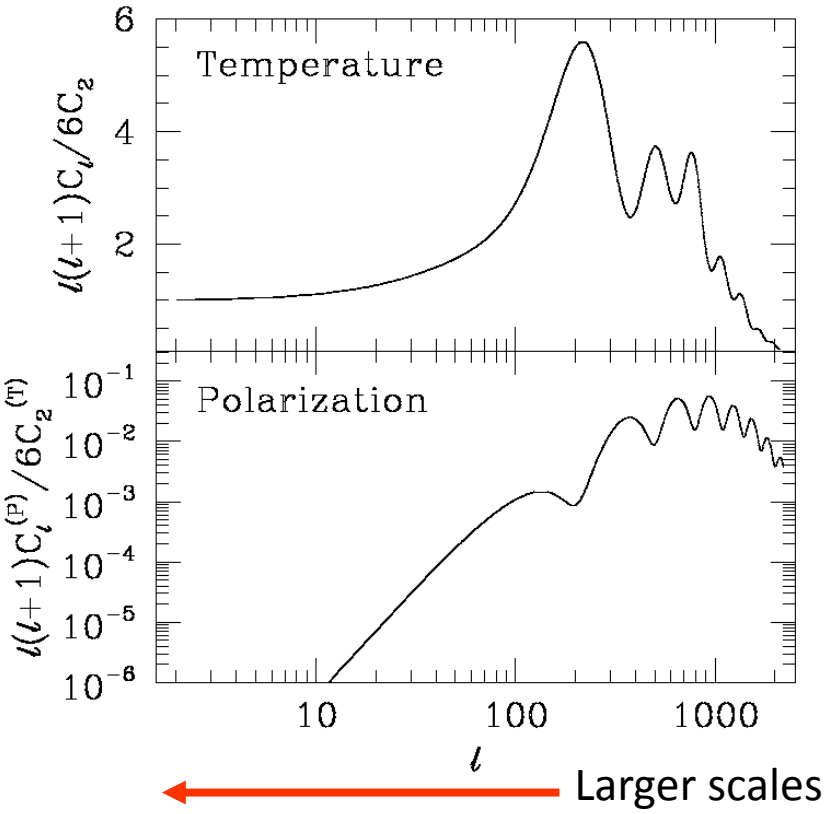

Small l's correspond to large angular scales, while large l's correspond to small angular scales.

We can correlate not only temperature but also polarization.

$$\left\langle \frac{\Delta T}{T}(\vec{\gamma}_1)\frac{\Delta T}{T}(\vec{\gamma}_2)\right\rangle = \frac{1}{2\pi}\sum_{\ell}(2\ell+1)C_\ell P_\ell(\vec{\gamma}_1\cdot\vec{\gamma}_2)$$

Physical Processes that Induce CMB Fluctuations

The primary anisotropies of CMB are induced by three principal mechanisms:

- Gravity (Sachs-Wolfe effect, regions with high density produce big gravitational redshift)
- Adiabatic density perturbations (regions with more photons are hotter)
- Doppler Effect (peculiar velocity of electrons on last scattering surface)

The anisotropies in temperature are modulated by the visibility function which is defined as the probability density that a photon is last scattered at redshift z:

$$\frac{\Delta T}{T}(\vec{n}) \doteq \int_0^\infty \left[g(z) \left(\Psi + \Theta_0 + \vec{n} \cdot \vec{v}_b \right) \right] dz$$

α

Gravity Adiabatic Doppler

Visibility function and fine structure constant

$$g(\eta) = \dot{\tau}\ e^{-\tau}$$

Rate of Scattering

$$\dot{\tau}(\eta) = n_e\, x_e\, a\sigma_T$$

Optical depth

$$\tau(\eta) = \int_{\eta}^{\eta_0} d\eta'\, n_e\, x_e\, a\sigma_T$$

$$x_e = \frac{n_e}{n_e + n_H}$$

We can see that the visibility function is peaked at the Epoch of Recombination.

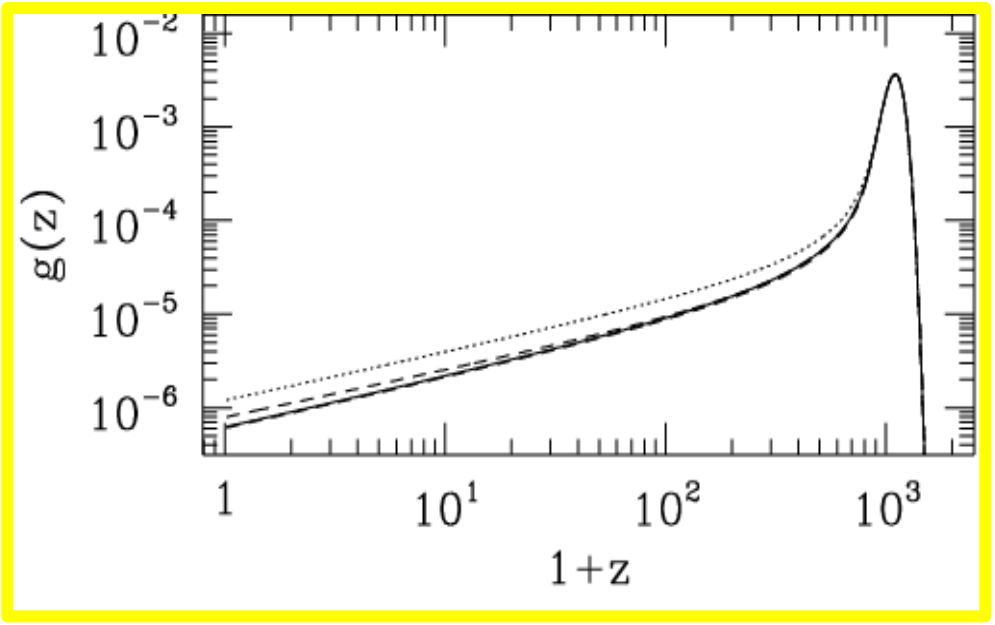

Thomson scattering cross section

$$\sigma_T = \frac{8\pi}{3}\frac{\hbar^2}{m_e^2 c^2}\alpha^2$$

Evolution of the free electron fraction with time

ionization coefficient

$$\beta_H \equiv R_H \left(\frac{2\pi m_e K_B T}{h^2} \right) e^{-B_2 / K_B T}$$

recombination coefficient

$$R_H \approx \sigma_{nl} f(B_n, T)$$

cross section of ionization

$$\sigma_{nl} \propto \alpha^{-1} m_e^{-2} f(h\nu / B_1)$$

$$\frac{dx_e}{dt} = C_H \left[\beta_H (1 - x_e) e^{-\frac{B_1 - B_2}{K_B T}} - R_H n_p x_e^2 \right]$$

$$C_H = \frac{1 + K\Lambda_{2s}(1 - x_e)}{1 + K(\beta_H + \Lambda_{2s})(1 - x_e)}$$

Rate of decay 2s a 1s $\quad \Lambda_{2s} \propto m_e \alpha^8$

Constant K $\quad K = n_e \lambda^3 / (8\pi H) \propto m_e^{-3} \alpha^{-6}$

Lyman-alpha $\quad \lambda_\alpha = 16\pi\hbar / (3 m_e c \alpha^2)$

Variation of free electron fraction

If we plot the free electron fraction versus the redshift, we can notice a different epoch of Recombination for different values of alpha. In particular if the fine structure constant α is smaller than the present value, then the Recombination takes place at smaller z.

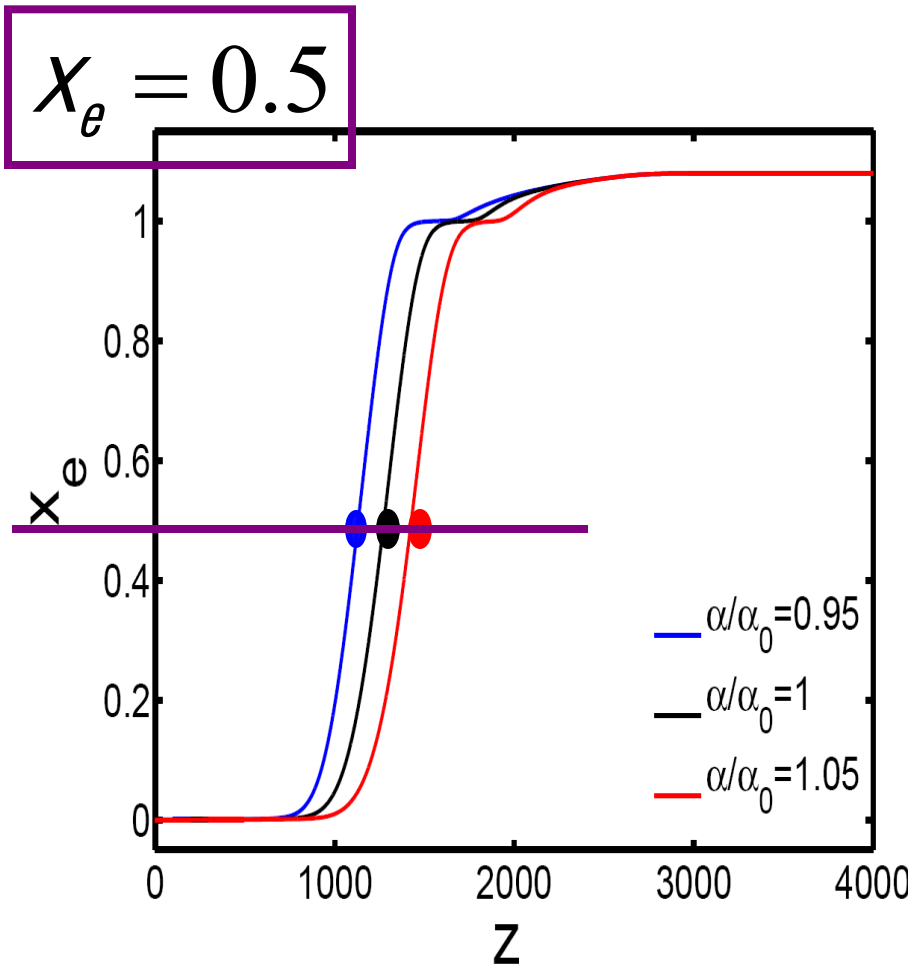

(see e.g. Avelino et al., Phys.Rev.D64:103505,2001)

Modifications caused by variations of the fine structure constant

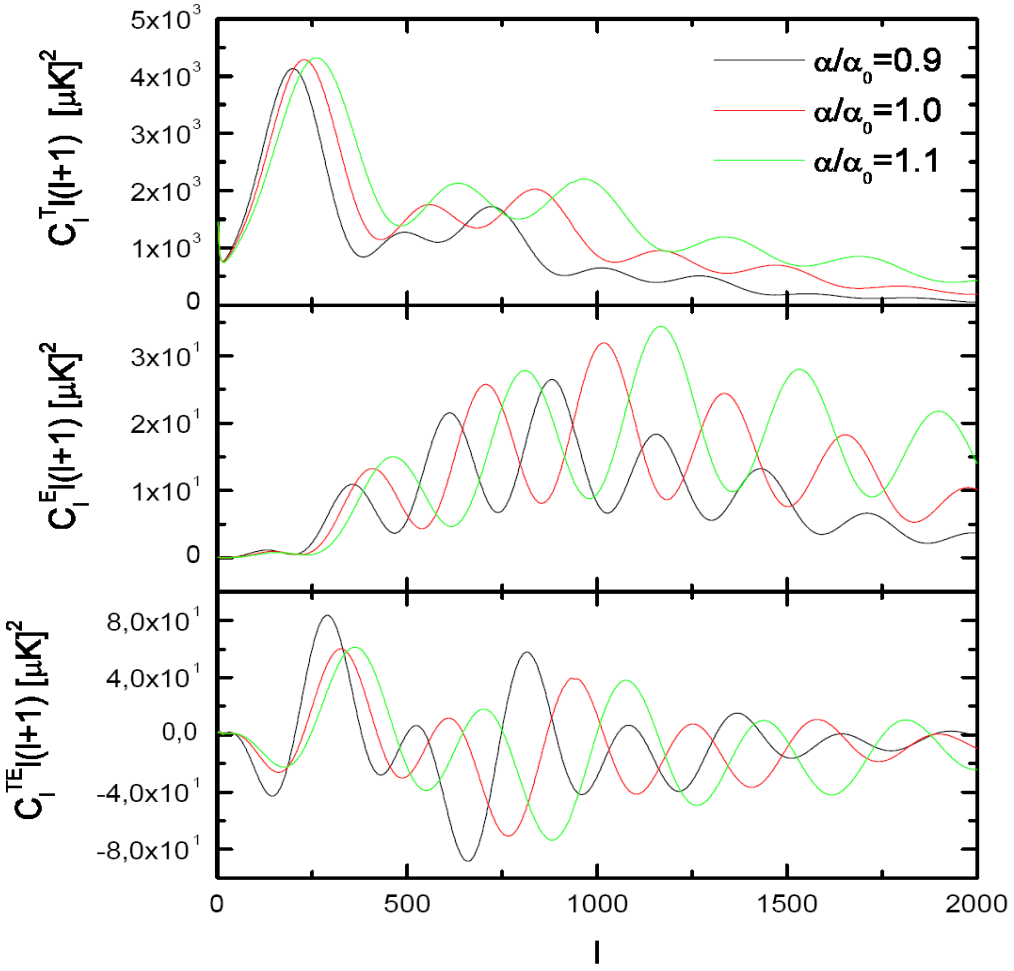

If the fine structure constant is $\alpha / \alpha_0 < 1$ recombination is delayed, the size of the horizon at recombination is larger and as a consequence the peaks of the CMB angular spectrum are shifted at lower l (larger angular scales).

Therefore, we can constrain variations in the fine structure constant at recombination by measuring CMB anisotropies !

New constraints on the variation of the fine structure constant

Menegoni, Galli, Bartlett, Martins, Melchiorri, arXiv:0909.3584v1
Physical Review D *80 08/302 (2009)*

We sample the following set of cosmological parameters from WMAP-5 years observations:

Baryonic density	$\Omega_b h^2$
Cold dark matter density	$\Omega_c h^2$
Hubble parameter	H_0
Scalar spectrum index	n_S
Optical depth	τ
Overall normalization of the spectrum	A_s
Variations on the fine structure constant	α / α_0

We also permit variations of the parameter of state w .

We use a method based on Monte Carlo Markov Chain (the algorithm of Metropolis-Hastings).

The results are given in the form of likelihood probability functions.

We are looking for possible degeneracies between the parameters.

We assume a flat universe.

Constraints on the fine structure constant

In this figure we show the 68% and 95% c.l. constraints on the α/α_0 vs Hubble constant for different datasets .

Experiment	α/α_0	68% c.l.	95% c.l.
WMAP-5	0.998	± 0.021	$^{+0.040}_{-0.041}$
All CMB	0.987	± 0.012	± 0.023
All CMB+ HST	1.001	± 0.007	± 0.014

TABLE I: Limits on α/α_0 from WMAP data only (first row), from a larger set of CMB experiments (second row), and from CMB plus the HST prior on the Hubble constant, $h = 0.748 \pm 0.036$ (third row). We report errors at 68% and 95% confidence level.

$\approx 0.7\%$

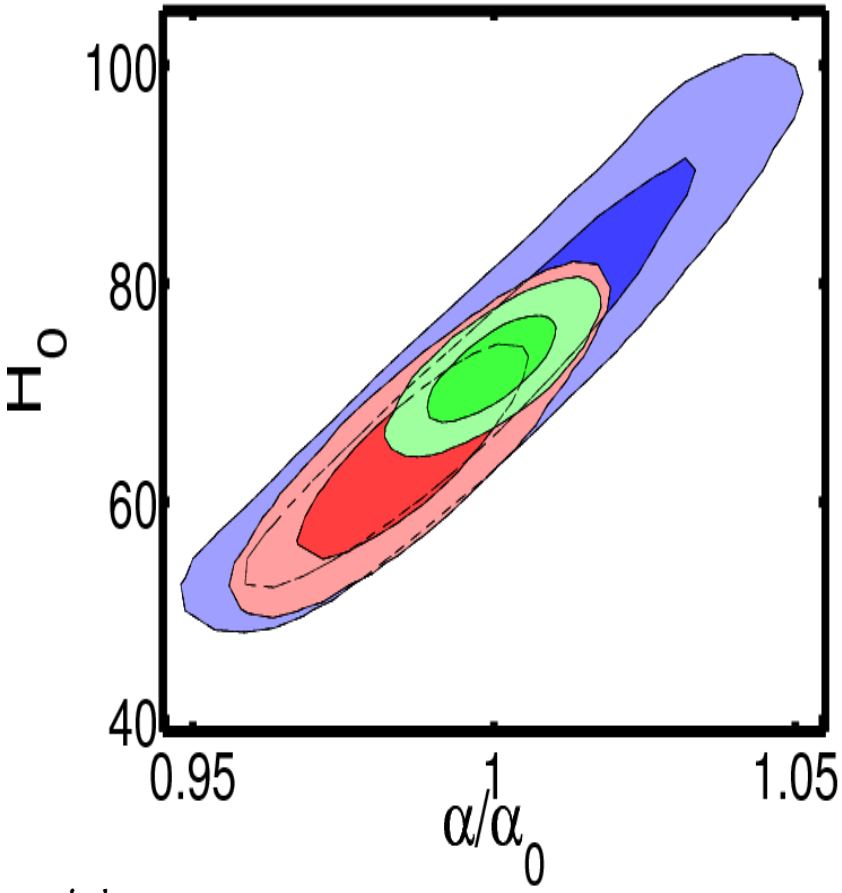

Menegoni, Galli, Bartlett, Martins, Melchiorri, arXiv:0909.3584v1
Physical Review D *80 08/302 (2009)*

Fine structure constant and the CMB damping scale

A variation of the effective number of relativistic degrees of freedom N_eff affects the value of the Hubble parameter H at recombination. This changes two very important scales in CMB anisotropy physics: the size of the sound horizon and the damping scale at recombination. An approximate expression for the damping scale is given by

$$r_d^2 = (2\pi)^2 \int_0^{a_*} \frac{da}{a^3 \sigma_T n_e H} \left[\frac{R^2 + \frac{16}{15}(1+R)}{6(1+R^2)} \right]$$

A change in H could be compensated by a change in the number density of free electrons in order to keep the same damping scale. Consequently, a change in the recombination process, motivated by some non-standard and unaccounted mechanism, could alter the current conclusions on Neff.

Constraints on N_eff and α WMAP7+ACBAR+ACT+HST+SPT+SDSS-DR7 data

Parameter	α/α_0	$\alpha/\alpha_0+N_{\rm eff}$	$\alpha/\alpha_0+N_{\rm eff}+Y_p$
$\Omega_b h^2$	0.0218 ± 0.0004	0.0224 ± 0.0005	0.0223 ± 0.0007
$\Omega_c h^2$	0.1144 ± 0.0034	0.1302 ± 0.0095	0.1303 ± 0.0094
τ	0.086 ± 0.014	0.088 ± 0.015	0.088 ± 0.016
H_0	68.9 ± 1.4	71.52 ± 2.0	71.8 ± 2.1
α/α_0	0.984 ± 0.005	0.990 ± 0.006	0.987 ± 0.014
n_s	0.976 ± 0.013	0.991 ± 0.015	0.992 ± 0.016
$\log[10^{10} A_s]$	3.193 ± 0.037	3.169 ± 0.040	3.167 ± 0.042
A_{SZ}	< 2.00	< 2.00	< 2.00
A_C	< 16.0	< 15.8	< 14.8
A_P	< 24.7	< 24.9	< 22.4
Ω_Λ	0.7137 ± 0.0070	0.7020 ± 0.0094	0.704 ± 0.013
Age/Gyr	13.76 ± 0.24	13.18 ± 0.38	13.15 ± 0.37
Ω_m	0.2863 ± 0.0070	0.2980 ± 0.0094	0.296 ± 0.013
σ_8	0.836 ± 0.023	0.862 ± 0.028	0.859 ± 0.034
z_{re}	10.7 ± 1.2	11.0 ± 1.3	11.0 ± 1.3
$N_{\rm eff}$	–	$4.10^{+0.24}_{-0.23}$	$4.19^{+0.31}_{-0.28}$
Y_p	–	–	0.215 ± 0.033
χ^2_{min}	7600.2	7596.8	7596.5

The dataset considered prefers a value of $\alpha/\alpha 0 < 1$ at more than 2-standard deviations when both the Neff and Yp are kept fixed at their standard values.

Allowing for variations in Neff significantly shifts the best fit value for $\alpha/\alpha 0$, which is now consistent with the standard value.

The largest effect on α comes however when also the helium abundance Yp is let to vary: the errors on α are almost doubled.

Likelihood contour plot for α/α_0 vs N_eff at 68% c.l. and 95% c.l. in the case of Y_p = 0.24 (red smaller contours) and Y_p allowed to vary (blue larger contours).

When helium abundance is Yp = 0.24 there is a clear but moderate degeneracy between α/α_0 and Neff. If Neff increased the H at recombination increases.

In order to keep the damping scale at the same value fixed by observations we need to decrease the x_e at recombination. This can be achieved by simply accelerating the recombination process. This effect is clearly obtained by an increase in α , so we see this degeneracy .

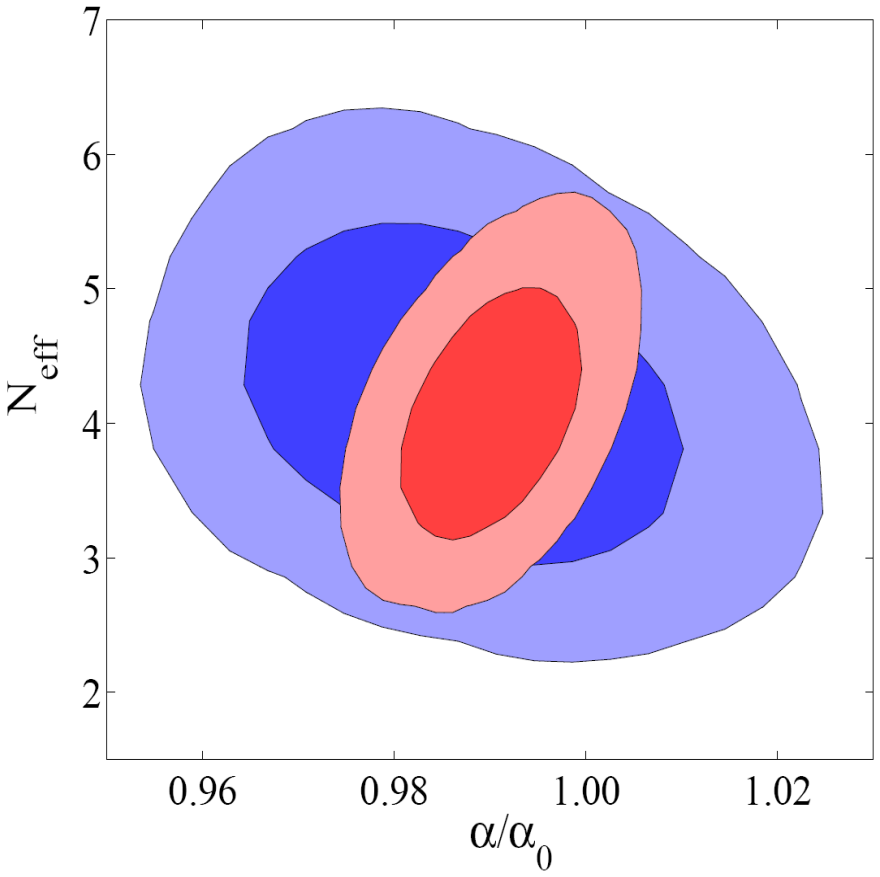

Eloisa Menegoni, Maria Archidiacono, Erminia Calabrese, Silvia Galli, C.J. A. P. Martins, Alessandro Melchiorri; PhysRevD vol. 85, id. 107301 (2012)

Future constraints on variations of α from combined CMB and weak lensing measurements

Experiment	Channel	FWHM	$\Delta T/T$
Planck	70	14′	4.7
	100	10′	2.5
	143	7.1′	2.2
$f_{sky} = 0.85$			

TABLE I. Planck-like experimental specifications. Channel frequency is given in GHz, the temperature sensitivity per pixel in $\mu K/K$, and FWHM (Full-Width at Half-Maximum) in arc-minutes. The polarization sensitivity is assumed as $\Delta E/E = \Delta B/B = \sqrt{2}\Delta T/T$.

Adding a noise spectrum to each fiducial spectra C_l:

$$N_l = W^{-1} \exp(l(l+1)/l^2{}_b)$$

We combined five quadratic estimators into a minimum variance estimator; the noise on the deflection field power spectrum C_dd ℓ produced by this estimator can be expressed:

$$N_l^{dd} = \frac{1}{\sum_{aa'bb'} (N_l^{aba'b'})^{-1}}$$

Galaxy weak lensing data

Using the Euclid specifications we produce mock datasets of convergence power spectra.

The 1σ uncertainty on the convergence power spectrum (P(ℓ)) can be expressed as:

$$\sigma_l = \sqrt{\frac{2}{(2l+1) f_{sky} \Delta_l}} \cdot \left(P(l) + \frac{\gamma_{rms}^2}{n_{gal}} \right)$$

$n_{gal}\,(arcmin^{-2})$	redshift	Sky Coverage (square degrees)	γ_{rms}
30	$0.5 < z < 2$	15000	0.22

TABLE II. Specifications for the Euclid like survey considered in this paper. The table shows the number of galaxies per square arcminute (n_{gal}), redshift range, sky coverage and intrinsic ellipticity (γ^2_{rms}) per component.

In our analysis we choose ℓ = 1 for the range $2 < \ell < 100$ and ℓ = 40 for $100 < \ell < 1500$. As at high ℓ the non-linear growth of structure is more relevant, the shape of the non-linear matter power spectra is more uncertain therefore, to exclude these scales, we choose ℓmax = 1500. We assume the galaxy distribution of Euclid survey to be of the form $n(z) \propto z^2 \exp(-(z/z_0)^{1.5})$ where z_0 is set by the median redshift of the sources, z_0 = z_m/1.41 with z_m = 0.9.

Matteo Martinelli, Eloisa Menegoni, Alessandro Melchiorri
Physical Review D, Vol.85, No.12, id. 123526 (2012).

	Planck		Planck+Euclid	
Model Parameter	Varying α/α_0	$\alpha/\alpha_0 = 1$	Varying α/α_0	$\alpha/\alpha_0 = 1$
$\Delta(\Omega_b h^2)$	0.00013	0.00013	0.00011	0.00010
$\Delta(\Omega_c h^2)$	0.0012	0.0010	0.00076	0.00061
$\Delta(\tau)$	0.0043	0.0042	0.0041	0.0029
$\Delta(n_s)$	0.0062	0.0031	0.0038	0.0027
$\Delta(\log[10^{10}A_s])$	0.019	0.013	0.0095	0.0092
$\Delta(H_0)$	0.76	0.43	0.34	0.31
$\Delta(\Omega_\Lambda)$	0.0063	0.0050	0.0034	0.0033
$\Delta(\alpha/\alpha_0)$	0.0018	–	0.0008	–

The Euclid future data improves the Planck constraint on α/α_0 by a factor of 2.6!!!

This is a significant improvement since for example, a 2σ detection by Planck for a variation of α could be confirmed by the inclusion of Euclid data at more than 5 standard deviation.

The precision achieved by a Planck+Euclid analysis is at the level of 5×10^{-4}, that could be in principle further increased by the inclusion of complementary datasets.

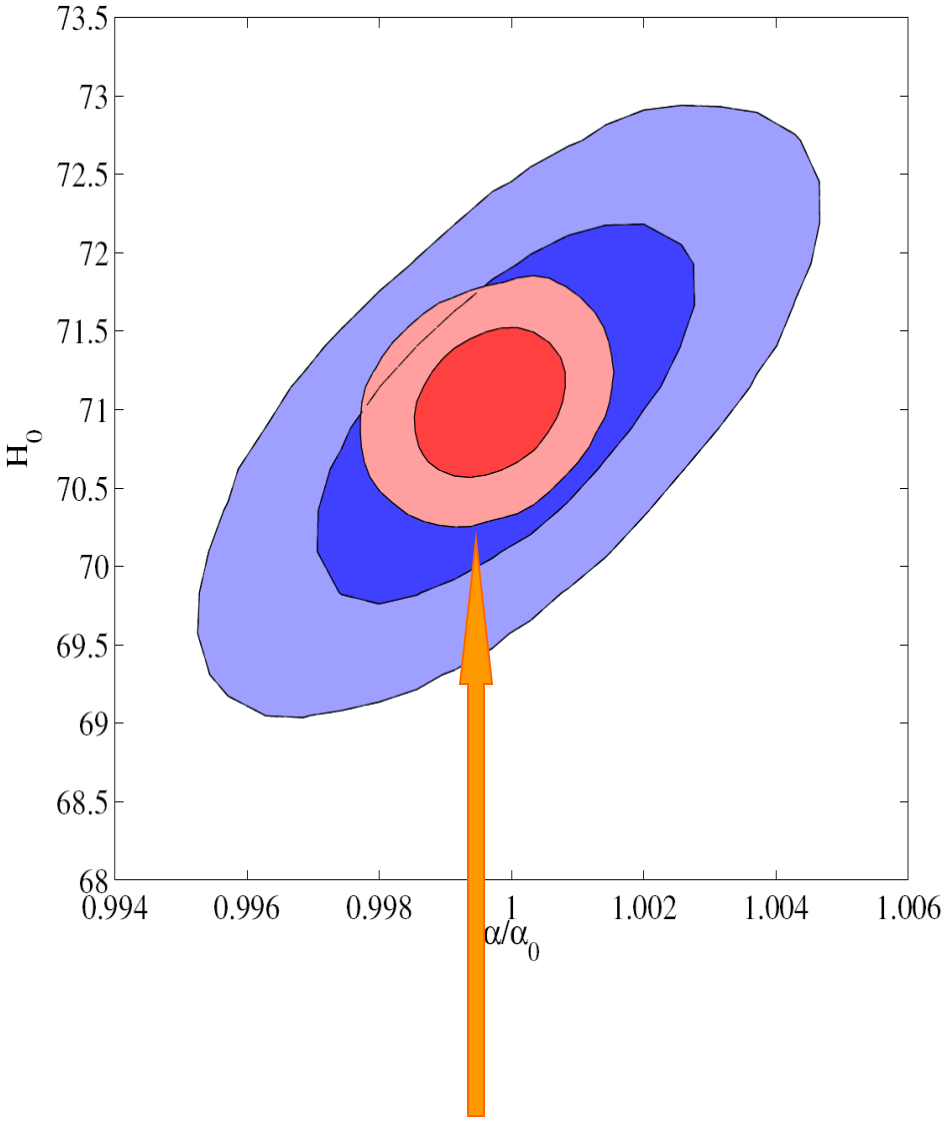

Planck+Euclid

There is a high level of correlation among $\alpha/\alpha 0$ and the parameters H_0 when only the Planck data is considered. This is also clearly shown in the plot of the 2-D likeihood contours at 68% and 95% c.l. between $\alpha/\alpha 0$ and H_0 . A larger/lower value for α is more consistent with observations with a larger/lower value for H_0.

Using EUCLID +PLANCK highlights a previously hidden degeneracy between $\alpha/\alpha 0$ and τ; both these parameters do not affect the convergence power spectrum, thus they are not measured by Euclid, but they are both correlated with other parameters, such as n_s whose constraints are improved through the analysis of weak lensing. This improvement on ns allows to clarify the degeneracy between $\alpha/\alpha 0$ and τ.

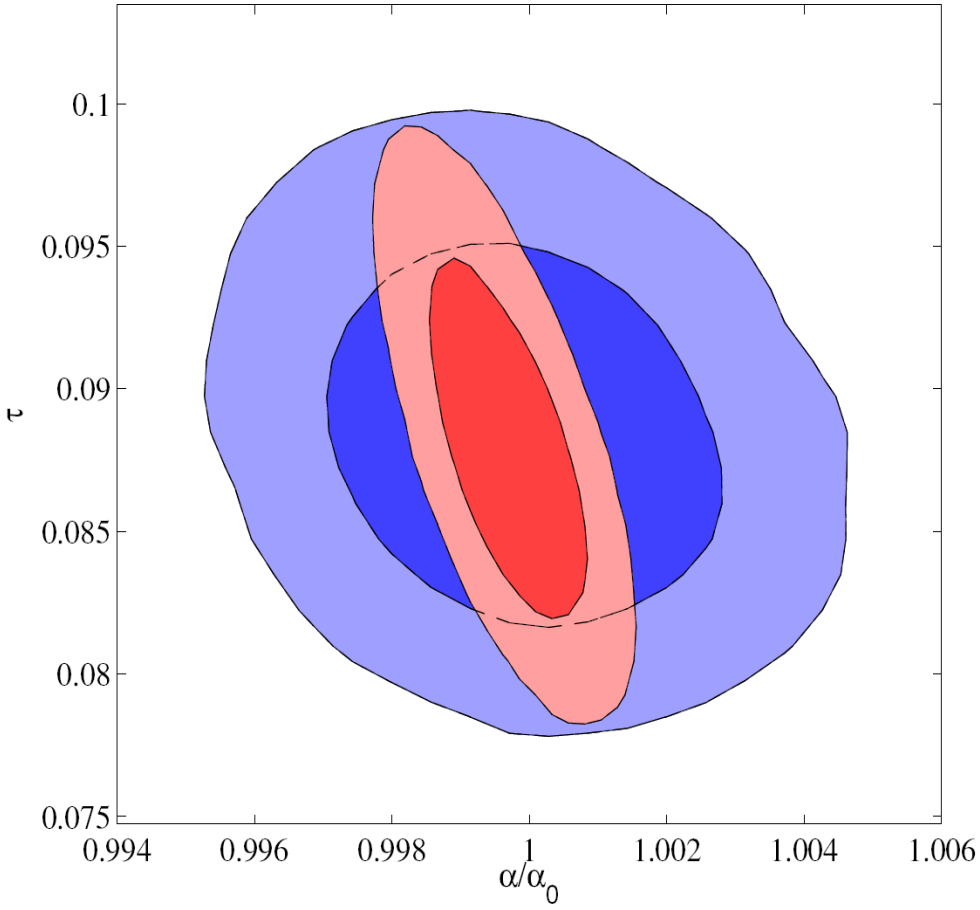

CONCLUSIONS:

We found a substantial agreement with the present value of the fine structure constant (we constrain variations at max of 2,5% at 68% level of confidence from WMAP-5 years and less than 0.7% when combined with HST observations).

There is no clear degeneracy between the early dark energy density parameter and the fine structure constant, and we can reach tighter constraints on the fine structure constant with the future experimental data (Planck).

From the latest CMB and ACT and SPT data, combined with other cosmological datasets and by assuming the standard value for Neff with primordial Helium abundance Yp = 0.24 the current data favours a lower value for the fine structure constant at more than 2 standard deviations with $\alpha/\alpha_0 = 0.984 \pm 0.005$. Clearly, further experimental confirmation of the result is needed. Planck is expected to have a sensitivity of $\delta(\alpha/\alpha_0) \approx 0.002$ and Neff=0.2.

Combining the data from Euclid+Planck experiments would provide a constraint on α of the order of $\alpha/\alpha_0 = 8 \times 10^{-4}$, significantly improving the constraints expected from Planck. we found that allowing in the analysis for variations in α has important impact in the determination of parameters as ns, H0 and τ from a Planck+Euclid analysis.

Constraints on the variations of the fine structure constant, EDE density parameter and on coupling

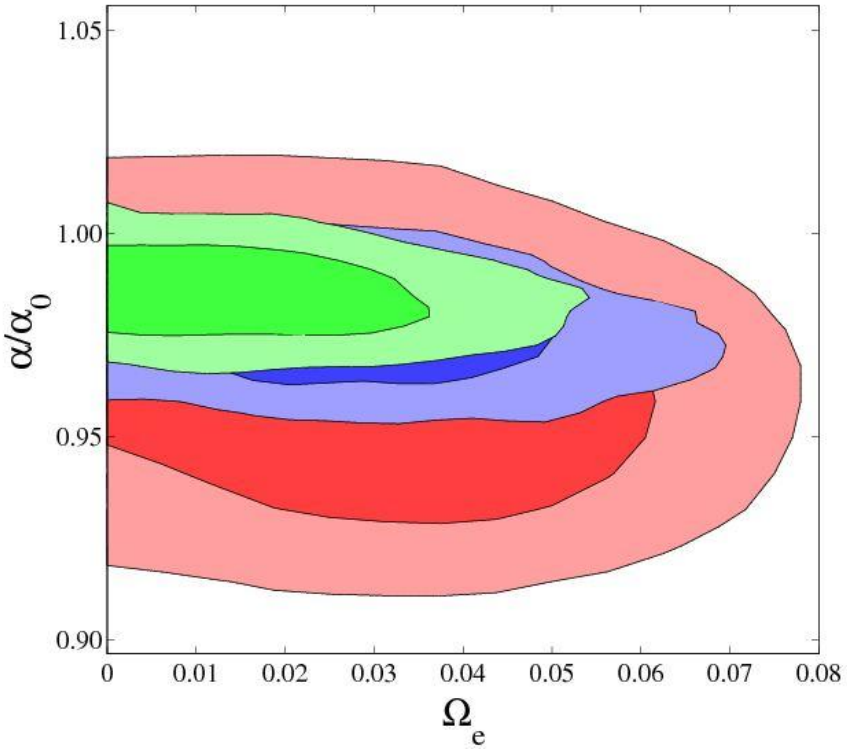

Experiment	α/α_0	Ω_e	ζ
WMAP7+HST	0.963 ± 0.044	< 0.064	< 0.047
WMAP7+ACT+HST	0.977 ± 0.010	< 0.051	< 0.028
WMAP7+ACT+HST+BAO	0.986 ± 0.014	< 0.043	< 0.024

Calabrese, Menegoni, Martins, Melchiorri and Rocha

Phys.Rev.D84:023518,2011